Research article

Investigation of climate change impact on the optimal operation of koka reservoir, upper awash watershed, Ethiopia

Sewmehon Sisay Fanta *, Mamuye Busier Yesuf, Tamene Adugna Demissie

Jimma University, Jimma Institute of Technology, Faculty of Civil and Environmental Engineering, Jimma, Ethiopia

A B S T R A C T

The objectives of this study were to predict the inflow and optimal operation of the Koka reservoir under the impact of climate change for the 2020s (2011–2040), 2050s (2041–2070), and 2080s (2071–2100) with respect to the reference period (1981–2010). The optimal elevation, storage, and hydropower capacity were modeled using the HEC-ResPRM, whereas the inflow to Koka reservoir was simulated using the calibrated SWAT model. Based on the result, the average annual inflow of the reference period was 139.675 Million Cubic Meter (MCM). However, from 2011 to 2100 an increase of +4.179% to +11.694 is expected. The inflow analysis at different flow regimes shows that the high flow may decline by (−28.528%) to (−22.856%) due to climate change. On the other hand, the low flow is projected to increase by (+78.407%) to (+90.401%) as compared to the low flow of the reference period. Therefore, the impact of climate change on the inflow to the Koka reservoir is positive. The study also indicates that the optimum values of elevation and storage capacity of the Koka reservoir during the reference period were 1590.771 m above mean sea level (a.m.s.l) and 1860.818 MCM, respectively. However, the optimum level and storage capacity are expected to change by (−0.016%) to (−0.039%) and (−2.677%) to (+6.164%), respectively from 2020s to 2080s as compared with their corresponding values during the reference period. On the other hand, the optimum power capacity during the reference period was 16.489 MCM, while it will likely fluctuates between (−0.948%) - (+0.386%) in the face of climate change. The study shows that the optimum elevation, storage, and power capacity were all higher than the corresponding observed values. However, the occurrence month of their peak value will likely shift due to climate change. The study can be used as a first-hand information for the development of reservoir operation guidelines that can account for the uncertainty caused by the impacts of climate change.

1. Introduction

Climate change has altered the duration, intensity, form, and timing of precipitation and a consistent increase in temperature [1–3]. Consequently, hydrological conditions are strongly influenced by the changing climatic variables [4,5]. Because of this, widespread flooding, fires, power fluctuation and reductions are serious global issues [6]. According to previous studies, it is predicted that the entire planet will experience the negative net effects of climate change [2,3,7,8]. On the other hand, the available climate and water resources greatly influence the amount of storage, inflow, and electricity generated by reservoirs. Therefore, climate change is a key

---

driver that can influences reservoir operation [4,9].

The operation of reservoir requires numerous decision variables, constraints, and competitive objectives [10]. Decisions about reservoir operation would be more challenging due to the uncertainty of inflow caused by the impacts of climate change. According to Hamududu and Killingtveit [6], climate change has a marginally favorable impacts on the global hydropower potential. However, the impacts of climate change on hydropower potential are not uniform throughout the world. The majority of the findings indicated the negative impact of climate change on reservoir operation [11–13]. However, Fan et al. [9] proved the favorable impact of climate change on the future hydropower potential of China. The hydropower potential of East Africa is also predicted to gradually increase under the impact of climate change [6].

The three well-known methods for dealing with reservoir stochasticity are explicit stochastic optimization (ESO), implicit stochastic optimization (ISO), and parameterization-simulation-optimization (SO). Both (parameterization-SO) and ISO can account the inflow uncertainties and provides rule curve in a more straightforward method than ESO [14]. Many researchers have successfully used the parameterization (SO) principle to develop reservoir rule curves under optimal reservoir operation [15]. The HEC-ResPRM is a simulation, and optimization model developed based on the parameterization SO technique.

Hydropower is the major source of Energy in Ethiopia. The country has an installed power capacity of 45,000MW, which is the second largest in Africa. However, 83% of the population do not have access to electricity [16]. Therefore, expanding hydropower projects and electricity generation are two of the four pillars of Ethiopia's Climate Resilience Green Economy (CRGE) [17,18]. Therefore, the Ethiopian government has planned to generate 22.14 Gigawatt (GW) of hydropower by the end of the 2030s [19]. According to the national master plan of the country, hydroelectric power will continue to be the largest energy source of the country due to its largest unexploited hydropower potential [20].

However, due to the influence of climate change, ensuring the consistency and reliability of power supply has become one of the most pressing issues [21]. On the other hand, the majority of reservoirs in Ethiopia are designed, maintained, and operated under the assumption of stationary historical climate data [10]. A study on the impact of climate change on hydroelectric power generation has received little attention, despite significant investment being made in hydropower projects. However, the water resources of Ethiopia are also highly vulnerable to inter-annual variability and climate change [1,2]. One of the observed adverse impacts of climate change on hydropower generation in Ethiopia was the prolonged and frequent blackouts from 2008 to 2010 throughout the country caused by an increase in power demand and a decrease in stream flow.

The Upper Awash watershed, the sub-watershed of Awash basin in Ethiopia, is also vulnerable to climate change. Recently, climate change has caused the watershed to experience frequent floods, droughts, and seasonal rainfall shifts [22]. The projected impact of climate change in the Upper Awash watershed also showed that it is expected to have a greater magnitude and direction than the influence already seen over the past three decades [22–25].

Few studies are done that showed the likely impact of climate change on the hydropower potential and hydroelectricity generation of Ethiopia. For instance, Bombelli et al. [21] investigated the impact of climate change on the hydroelectric power generating capacity of GERD and GIBE reservoirs. To simulate the ideal power production and the future hydrological balance, they used Poli-Hydro and Poli-Power models. According to the finding, the energy production of the GERD reservoir exhibited both a rising and a declining signal at the end of the 2050–2059 and 2090–2099 centuries, respectively, whereas the power capacity of the GIBE–III hydropower showed an increasing signal. Another study by Mirani et al. [18] revealed that the hydropower potential of Kessem reservoir in Ethiopia showed a declining trend under the influence of climate. Adera and Alfredsen [16] also investigated how the Tekeze hydropower reservoir might perform under the influence of climate change. The inflow and power capacity were simulated using the HVB and nMAG models, respectively. The finding indicated that future energy production is likely to increase. Another study conducted by Leta et al. (26) showed that Land Use/Land Cover (LU/LC) and climate change have marginally favorable impact on the optimal operation of Nash reservoir in Ethiopia.

The impact of climate change on the water resources of Upper Awash watershed is indicated by Previous studies [22,25]. To the best knowledge of the authors, the hydropower capacity and optimal operation of Koka reservoir in the face of climate change is not studied yet. The rule curve developed by Halcrow [26] is extrapolated to compute the current monthly storage-elevation- area curve [27,28]. This rule curve was based on historical data without accounting for temporal fluctuations in hydro meteorological variables. Because of this, the Koka hydropower reservoir is typically used at less than its installed capacity. Therefore, it is crucial to quantify the expected consequences of climate change for the reservoir to operate optimally.

Therefore, the objectives of this study are: (1) to predict the monthly inflow of the Upper Awash watershed in the face of climate change and (2) to investigate the likely impact of climate change on the optimal operation of the Koka reservoir. During the reference period, the inflow of the Koka reservoir was simulated using the observed climate and stream flow, whereas from 2011 to 2100, the monthly inflow of the Koka reservoir was simulated using the future climate data projected by the ensemble output of RCMs. The optimum elevation, storage, and hydropower capacity of the Koka reservoir was simulated using the inflow as input data in HEC-ResPRM. The novel finding of the study is the investigation of the impact of climate change on various flow regimes for Koka reservoir inflow. The study's novel approach also includes the use of penalty functions and physical constraints to predict optimal reservoir operation.

The finding of this study can assist decision-makers and dam operators in gaining a thorough understanding of choices for the Koka reservoir's optimal operation.

2. Methodology

2.1. Description of the study area

The Upper Awash watershed is part of the Awash River basin which is located in the Northwest rift valley around the central part of Ethiopia. Geographically, the Upper Awash watershed is found between 37°57′–39°13′ E longitude and 8°9′–9°18′ N latitude. The watershed has a total area of 11, 500 km^2. The elevation of the watershed ranges from 1587 m to 355 m a.m.s.l. The Koka reservoir is situated between 8° 18″ and 8° 29″ N latitude and 39° 00″ to 39° 10″ E longitude. The reservoir has a total storage capacity of 1850 MCM and a useable storage capacity of 1650 MCM. The maximum and minimum operational levels of the reservoir are 1590.7 m, and 1580.7 m a.m.s.l, respectively. The firm and installed capacities of the power plant are 43.2 Megawatt (MW) and 34.5 MW at working heads of 32 m and 40 m, respectively. Fig. 1 shows the location map of Upper Awash watershed and Koka reservoir.

There are large mechanized and private irrigated agricultural farms in Upper Awash watershed [28,29]. The LU/LC data analysis indicates that 83.04% of the watershed was used for agriculture during the reference period of the study. As shown in Fig. 2 (a), the intensively and moderately cultivated portion of the watershed dominated the LU/LC of Upper Awash watershed. Based on the FAO soil classification system, the soil data analysis indicated that 45.686% of the watershed is covered by pellic vertisols, which is mainly distributed in the central highland, whereas the minimum portion of the watershed is covered by Orthic luvisols (0.562%). Fig. 2 shows the spatial distribution of soil and LU/LC types of the watershed.

The climate condition of the watershed is dominated by humid subtropical to semiarid. The rainfall data analysis from 1981 to 2010 indicated that the annual rainfall of the watershed was 995.763 mm. Based on the seasonal rainfall distribution, 69.544% of rainfall occurred between July and September. The short rainy season (March to April) contributed 24.525% of the annual rainfall. The remaining amount of annual rainfall occurred during the driest season (October to January) of Ethiopia. As shown in Fig. 3, the maximum and minimum rainfall values were 227.671 mm and 7.996 mm, which were observed in August and December, respectively. The observed temperature data analysis also shows that the mean annual minimum and maximum temperature values of the watershed were 10.673 °C and 23.591 °C, respectively.

2.2. Data collection and analysis

Spatial data (LU/LC, soil, and DEM), hydro-meteorological data i. e rainfall, temperature, wind speed, relative humidity, sunshine hour, and stream flow, and physical and operational data of the Koka reservoir were the main data used for this study. The LU/LC, soil and stream flow data were obtained from the office of Ministry of Water, Irrigation, and Electricity of Ethiopia. A DEM with a resolution of 12.5 m by 12.5 m was obtained from the Alaska Satellite Facility Service (http://www.vertex.daac.asf.alaska). The storage-area-elevation curve, monthly observed power from 2011 to 2021, turbine efficiency curve, the dimensions and different components of the reservoir were obtained from Ethiopian Electric Power Corporation, site observation and information collected from the project managers.
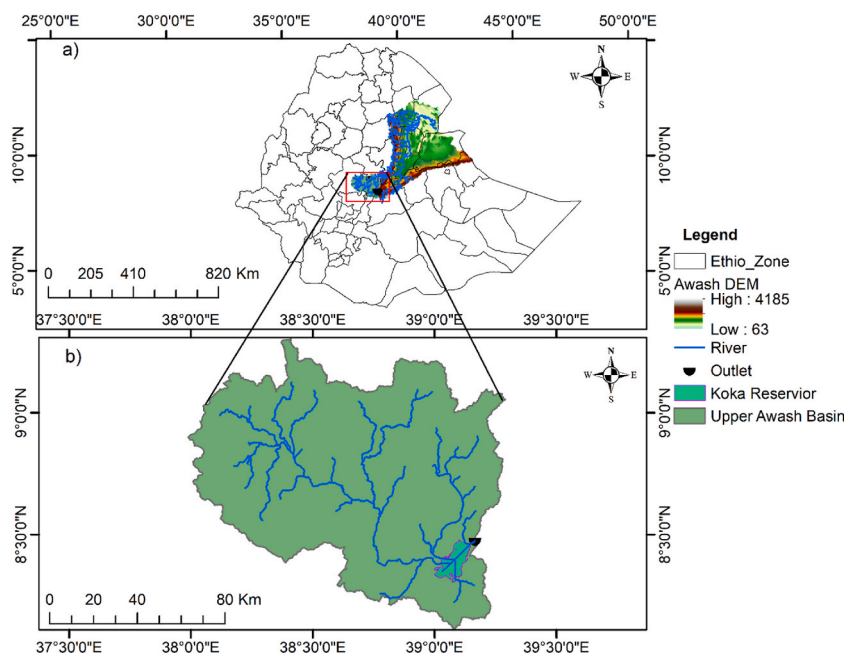

Fig. 1. Location map of the Upper Awash watershed; a) Administrative Zone of Ethiopia and Awash River basin, b) Upper Awash Basin.
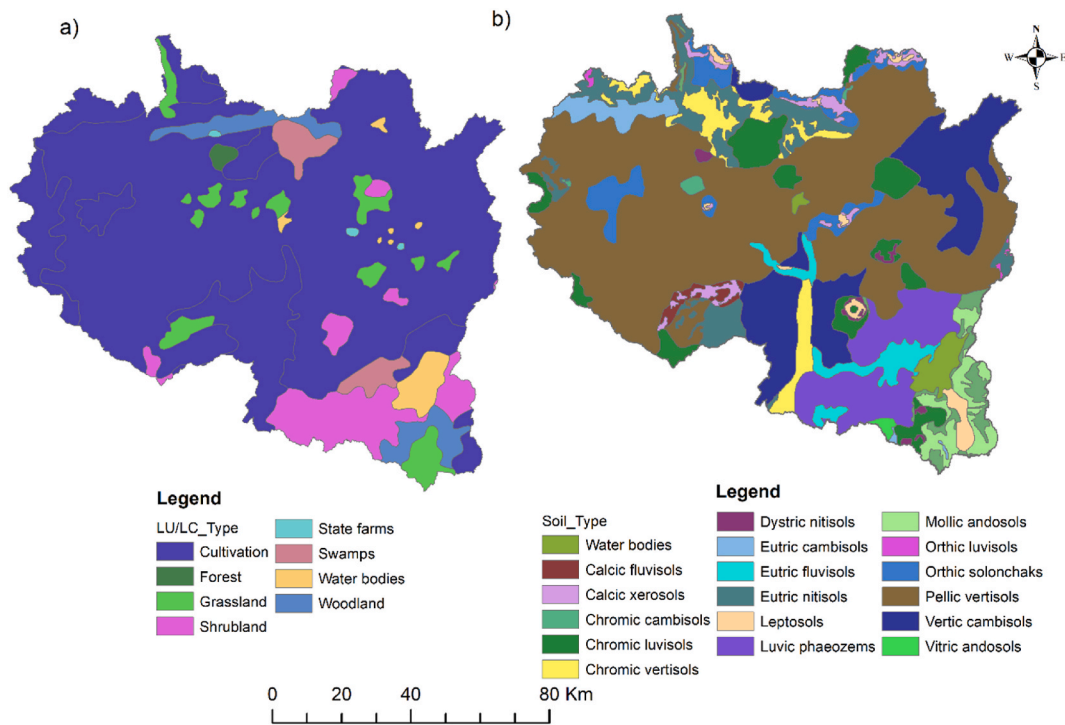
Fig. 2. Spatial distribution of LU/LC and soil type of the Upper Awash watershed; a) LU/LC type, b) Soil type.
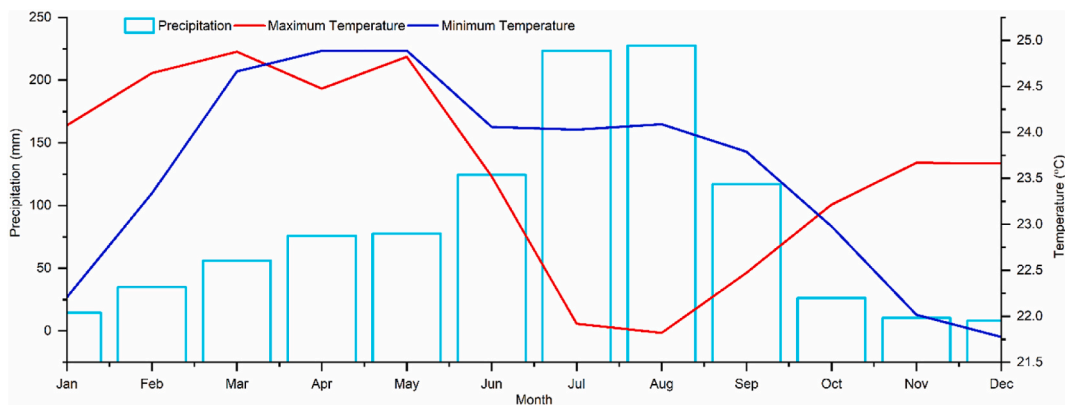

Fig. 3. Monthly distribution of rainfall, maximum and minimum temperature.

The monthly meteorological data from 1981 to 2010 was obtained from the office of National Meteorological Agency of Ethiopia. Each Hydrologic Response Unit (HRU) in SWAT model receives its climate information from the nearest climate station. Therefore, in addition to the quality and data availability the selection of meteorological stations, among the available stations, were based on their proportional distance from each other and the density of gauge distribution. Accordingly, nine meteorological stations having proportional distance to each other was taken were selected (Table 1). Furthermore, to preserve the data quality, stations with more than 10% of missing data were excluded based on the analysis of the climate data.

The primary water sources of Koka reservoir are Mojo and Hombole rivers. However, the Mojo and Hombole gauging stations, which measure the stream flow of the respective rivers, are located at 42 km and 35 km away from the inlet of the Koka reservoir, respectively. There is no any other tributary, LU/LC change or diversion structures between the two stations and the inflow point of the Koka reservoir. Therefore, transferring the stream flow from the two gauges toward the inlet of Koka reservoir is not needed. However, areal scaling should be used to use the time series data form the two stations as inflow to Koka reservoir. Therefore, in order to estimate the inflow of the Koka reservoir from the two stations, Halcorw (27) developed a rainfall-area-runoff regression equation (Eq. (1)).

$$\text{Inflow} = 1.065 * Q_{\text{Hombole}} + 1.18 * Q_{\text{Mojo}} \tag{1}$$

Table 1
Summary of the selected meteorological stations.

I.D.	Name	Lat (Deg)	Long (Deg)	Elevation (m)
1	Addis Abeba	9.01891	38.7475	2355
2	Bulbula	7.72	38.6525	1606
3	Boneya	8.48	38.39	2879
4	Ginchi	9.01667	38.1333	2492
5	Hombole	8.368167	38.78	1860
6	KokaDam	8.471	39.157	1661
7	Sebeta	8.93	38.63	2213
8	Sendafa	9.152167	39.0215	2482
9	Tulubolo	8.658	38.211	2310

Where $Q_{Homoble}$ and Q_{Mojo} represents the monthly observed flow at Hombole and Mojo gauging stations, respectively. Hence, in this study, the observed inflow of the Koka reservoir for the reference period was calculated using Eq. (1).

Currently, climate data simulated by GCMs and RCMs are the primary data sources for future studies on climate change impacts and adaptation [30]. However, GCMs have their own limitation regarding the model formulation, spatial and numerical resolution, initial assumptions, and local topographic effect. According to Doulabian et al. [31], local scale climate and hydrologic process are not well represented by GCMs due to their low resolution. To capture the details of the hydrologic process at local scale, RCMs are dynamically downscaled from GCMs at a resolution (from 25 km to 50 km) [32]. Topography and local scale features needed to assess the local climate conditions at the watershed scale are better represented in RCMs due to their high spatial resolution. However, RCMs also have their own uncertainty in reproducing climate projections due to the limitations inherited from GCMs [33]. As a result, no single RCM is considered the best and can accurately replicate climate projections. Using the multimodal ensemble output, according to Faramarzi et al. [33]; Reda et al. [34] and Dibaba et al. [35], can minimize the uncertainty of climate projection. Therefore, in this study, the climate data from 2011 to 2100 was obtained from the multimodal ensemble output of DMI-HIRHAM5, KNMI-RACMO22T, CLMcom-CCLM4-8-17, RCA4, REMO2009, and CanRCM4 under the RCP4.5 and RCP8.5 forcing scenarios. The first four RCMs are forced by ICHEC-EC-EARTH, whereas the last RCM (CanRCM4) is forced by CCCma.CCCma-CanESM2. According to previous studies conducted in the different climatic zones of Ethiopia [19,25,36,37], the performance of the selected RCMs is adequate and acceptable.

2.3. SWAT model description and setup

The SWAT model is a semi-distributed and continuous time-based hydrological model used to simulate the hydrological processes and water quality at various watershed scales [38–41]. Due to its user-friendly interface, open-source code and extensive regional adaptation, capability, and computational efficiency, the SWAT model is successfully applied for continuous simulations of flow, soil erosion, sediment yield, water quality and nutrient transport in different types of watersheds, irrespective of their size, complexity and climatic condition [5,19]. In this study, the main reasons for choosing the SWAT model are (1) The spatial and non-spatial data required by the model are available at the desired resolution (2) The model and its manual are non-commercial. (3) The performance of the model for surface runoff simulation in different watersheds of Ethiopia is appreciated and recommended [5,19,42–44]. (4) The continuous time-based properties of the SWAT model can allow runoff prediction at user defined temporal resolution.

The different hydrological components in the SWAT model are computed using water balance equations, whereas, surface runoff and peak discharge of the watershed are computed by the modified Soil Conservation Service Curve Number (SCS–CN) and modified rational method, respectively which are available in Arnold [45]. The SCS-CN equation simulates the surface runoff using LU/LC, soil, slope, antecedent moisture condition and climate of the watershed at the HRU level. There is no conclusive guideline regarding the number of HRUs for a given watershed. However, according to Arnold et al. (46), physiographic characteristics (Soil, LU/LC, slope, and moisture condition) should be considered during the spatial discretization of the watershed. Accordingly, considering the spatial variation of physiographic characteristics, the Upper Awash watershed was divided into 41 sub-basins and 195 HRUs.

Sensitivity analysis, model calibration and validation were performed using the Sequential Uncertainty FItting version 2 (SUFI 2) in the SWAT-CUP 2012 program [45]. Sensitivity analysis was conducted to determine the most influential watershed parameters for surface runoff. The most influential watershed parameter is determined based on the level of agreement between the simulated and observed runoff at different Parameter optimization trial. However, a random selection of parameters and fixing their initial value from the allowable range provided by the SWAT model may not allow us to obtain the required level of agreement between the simulated and observed runoff at a minimum number of iterations [46]. Therefore, previous literatures [17,22,40] were reviewed to determine the type of parameters and their initial values used for the SWAT model calibration.

The result of sensitivity analysis showed that The CNII is the most sensitive parameter for surface runoff in the Upper Awash watershed. This is because most runoff causative factors (LU/LC, topography, and soil) are lumped by a single curve number value. Hence, a minor change of its initial value can bring a significant change on surface runoff. Furthermore, surface runoff lag time (SURLAG) also depends on the curve number, the longest flow path of the river, and basin slope of the basin. Hence, the sensitivity of SURLAG also demonstrates that the basin slope is the major cause of surface runoff. The sensitivity analysis of this finding is also in accordance with the finding of Mekonnen et al. [17]; Dibaba et al. [19]; Amin and Nuru [47]. Table 2 shows the most sensitive, fitted, minimum, and maximum values of the selected parameters. The degree of sensitivity was measured by t-stat and p-value. Accordingly, a parameter having a high t-value and the low p-value is sensitive.

Table 2
Values of optimum surface runoff parameters of the Upper Awash watershed.

Parameter short name	Description	t-Stat	P-Value	Fitted Value	Minimum value	Maximum value
R: CN2.mgt	SCS runoff curve number	4.041	0.000	0.129	−0.053	0.313
R: SURLAG.bsn	Surface runoff lag time	1.660	0.098	7.446	1.443	20.384
V: ALPHA_BF.gw	Base flow alpha factor	1.081	0.280	0.178	0.046	0.299
R: CH_N2.rte	Manning's "n" value for the main channel	0.303	0.762	0.008	0.007	0.009
A: SOL_K.sol	Saturated hydraulic conductivity	−0.127	0.899	0.794	0.768	0.874
R: CH_K2.rte	Effective hydraulic conductivity in main channel alluvium	−0.634	0.527	5.363	4.248	5.392
A:SOL_Z(..).sol	Depth from soil surface to bottom of layer.	−0.691	0.490	17.961	14.785	24.073
V: GWQMN.gw	Threshold depth of water in the shallow aquifer required for return flow to occur (mm)	−1.010	0.313	0.765	0.707	0.787
R: SOL_AWC.sol	Available water capacity of the soil layer.	−1.361	0.174	−0.022	−0.054	−0.018
V: GW_DELAY.gw	Groundwater delay (days).	−1.491	0.137	44.241	38.474	46.869

The identifier code behind the short name of each parameter indicates the type of change to be applied to the initial value of the parameter. (R) indicates multiplying the initial value by the fitted value then add or subtract the final value from the initial value, (V) indicates the direct replacement of the optimum parameter's value by the initial value of the parameter, (A) denotes adding the optimum and initial parameter's value.

The model performance was evaluated using 17 years (from 1981 to 1998), and 12 years (from 1999 to 2010) of stream flow data during the model calibration and validation phases, respectively. The widely used objective functions i. e the modified Coefficient of Determination (bR^2), the Nash and Sutclif Efficiency (NSE), the Percent Bias (PBIAS (%)), the Kling–Gupta efficiency (KGE), and the ratio of root-mean-square error to the standard deviation of the data (RSR) were used to measure the performance of the SWAT model for the monthly runoff simulation of Upper Awash watershed. The equations, descriptions, and their acceptable range of objective functions are available in Moriasi et al. [48]; Verma et al. [49], and Bekele et al. [50].

2.4. HEC-ResPRM description and setup

HEC-ResPRM is an integration of the simulation (HEC-ResSim) and optimization (HEC-PRM) models used to study a single or multi-objective reservoir operation [14]. The HEC-PRM is a generalized program intended to perform the deterministic network flow optimization of reservoir operation [15]. Penalty function is crucial to study the optimal operation of reservoir. Reservoir operation that deviates from the target value should be penalized. Hence, the penalty function associates a penalty or reward for inflow, storage/elevation, and outflow. It is possible to address the multi-objective nature of reservoir operation by allowing any number of penalty functions [51]. Accordingly, the objective of reservoir optimization is to bring the system operation closer to the target operation. The HEC-ResPRM uses the primal network simplex method to find the minimum-cost path, assigned with minimum penalty function in the network [10]. Then, it solves the optimization problem using network flow programming (Eq. (2) to Eq. (4), which is a special form of linear programming algorithm in HEC-ResPRM to simulate the optimal solution of flow, storage, release, and hydropower [52].

In this study, an arc represents a reach of stream between two physically adjacent nodes. The node represents the junction of two or more networked arc, the starting point of inflow and outflow of the Koka reservoir. l_l and u_l are the minimum and maximum monthly inflow to the Koka reservoir.

$$\text{Minimize} : \sum l \in A \, c_l q_l \tag{2}$$

$$\text{Subject to} : \sum j \in o_i q_j - \sum k \in I_i q_k = 0; \text{for all } i \in N \tag{3}$$

$$l_l \le q_l \le u_l; \text{ for all } l \in A \tag{4}$$

Where A denotes a set of all arcs in the network, c_1 is a weighting factor assigned for along arc "l", ql is the flow along arc "l", O_i denotes a sets of all arcs that originates from node "i", I_i denotes the inflow arc, l_l and u_l are the lower and upper bound on flow along arc "l", N is set of all nodes in the network, qk is a multiplier (gain) for arc "l".

The mathematical expression for storage, release, and excess spill constraints for this study are given in Eqs. (5)–(7), respectively. However, the optimum storage at the end of each month is calculated using the water balance equation (Eq. (8)) in HEC-ResPRM under constraints and penalty functions as input boundary conditions.

Constraints on Storage

$$S_{\min} \le S_t \le S_{\max}, \forall t = 1 \text{ to } T \tag{5}$$

Release constraint

$$R_{min} \leq R_t \leq R_{max}, \forall t = 1 \text{ to } T \tag{6}$$

Spill constraint

$$Spt = \begin{cases} S_t + Q_t - R_t - S_{max}, \text{if } S_t + Q_t - R_t > S_{max} \\ 0 \text{ if } S_t + Q_t - R_t \leq {}_{max}S \end{cases} \forall t = 1 \text{ to } T \tag{7}$$

Water balance equation in a reservoir

$$S_{t+1} = S_t + Q_t - Q_{out} - Q_{loss} \forall t = 1 \text{ to } T \tag{8}$$

Where S_{min} and S_{max} denote the initial and maximum reservoir storage capacity, S_t, denotes the optimized storage capacity of the Koka reservoir throughout the operation period, T, R_{min} and R_{max} represents the minimum, and maximum allowable release, Rt denotes the optimized release during the operation period t, Q_t, Q_{out}, and Q_{loss} denotes the inflow (during the operation period, t), outflow and volume of water lost in the form of evaporation, respectively.

The monthly evapotranspiration in this study was computed using the modified FAO penman -Monteith equation available in Allen et al. [53]. Then, the evaporation at the maximum area of the Koka reservoir was computed by using Eq. (9).

$$V_{loss} = E_t * A \tag{9}$$

Where V_{loss}, E_t and A represent the volume of water lost by evaporation from the Koka reservoir (m^3), the evapotranspiration (mm), and the area of the reservoir. The volume of water lost by evaporation was computed at the maximum area of the reservoir.

The monthly irrigation water demand was computed using Cropwat8.1 software using irrigation area, soil, climate, and crop information. As shown in Table 3, the sum of minimum and maximum environmental and irrigation flow requirements is 11.650 MCM and 114.482 MCM, respectively. Therefore, the optimum release should be between these upper and lower values throughout the reservoir operation period. The current irrigated area in the Upper Awash watershed is 30,000 ha. However, detail studies regarding the future expansion of the irrigation area, irrigation infrastructures, and economic feasibility are not available. Accordingly, the estimated environmental and crop water demand for the reference period was not changed throughout study period.

3. Results and discussion

3.1. SWAT model calibration and validation result

The monthly average observed and simulated runoff values during the calibration and validation periods were 145.47 m^3/s (148.16 m^3/s) and 72.14 m^3/s (67.570 m^3/s), respectively, while the standard deviation values were 202.220 m^3/s (224.860 m^3/s) and 98.090 m^3/s (108.440 m^3/s), respectively. The result shows that the average and standard deviation values of the simulated flow agreed with their corresponding values of the observed flow. Hence, the monthly simulated runoff during dry and rainy periods was complimentary to the observed flow. On the other hand, mean annual rainfall values during the calibration and validation periods were 1066.332 mm and 889.071 mm, respectively. Accordingly, the acceptable values of statistical tests of error functions showed that the percentage of rainfall appearing as surface runoff is quite reasonable. Therefore, magnitude and pattern of the simulated surface runoff were consistent with the temporal magnitude and distribution of rainfall. The summary statistics of the model performance are shown in Table 4. According to Moriasis et al. [48] and Pechlivanidis et al. [54], the values of a statistical test of error functions are within the acceptable range.

Table 3

The long-term monthly average environmental, irrigation requirement and evaporation of the Upper Awash watershed.

Month	Environmental flow (MCM)	Flow for irrigation (MCM)	Evaporation (MCM)
Jan	2.542	43.630	32.267
Feb	2.532	42.946	28.167
Mar	2.592	36.645	36.833
Apr	2.592	44.404	28.367
May	2.552	44.444	38.867
Jun	1.292	10.358	41.567
Jul	1.892	12.461	30.967
Aug	1.592	13.586	17.033
Sep	2.592	30.475	38.400
Oct	2.592	87.327	53.800
Nov	2.592	111.890	35.300
Dec	2.572	95.739	35.967

Table 4
Optimum values of objective functions during the calibration and validation periods.

Objective functions	Calibration period	Validation period
bR^2	0.671	0.840
NSE	0.820	0.840
PBIAS (%)	1.817	−6.642
KGE	0.860	0.860
RSR	0.420	0.400
PEP (%)	19.084	20.836
MAE (m^3/s)	2.692	4.493
Mean_sim (Mean_obs) (m^3/s)	145.470 (148.160)	72.140 (67.570)
StdDev_sim (StdDev_obs) (m^3/s)	202.220 (224.860)	98.090 (108.440)

The visual evaluation of the observed and simulated monthly runoff hydrographs (Fig. 4) also reveals that the signal and pattern of the simulated runoff closely matches with the observed runoff. Thus, a graphical and statistical evaluation of the observed and simulated runoff demonstrated the suitability of the SWAT model for the monthly runoff simulation of the Upper Awash watershed. The probable reasons for the good performance of the SWAT model could be (1) the initial watershed parameters for the SWAT model were obtained from previously calibrated hydrological models [17,22,25,29,47] in the Upper Awash watershed and on the entire Awash basin. (2) The SCS-CN method has been proved to perform better in Agricultural watersheds. In this regard, 83.040% of the Upper Awash watershed was used for agriculture from 1981 to 2010.

However, there was a slight difference between the simulated and observed runoff values during the calibration and validation periods. The significant deviation of the simulated runoff from the observed runoff was toward the higher extreme values (Fig. 4). During the calibration and validation periods, the observed peak discharge values were 1441 m^3/s and 542.041 m^3/s, respectively. However, the simulated peak discharge values during the calibration and validation periods were underestimated by −19.084% and −20.836%, respectively. Hence, the peak discharge was not well simulated by the model as compared to the average runoff. This is a typical weakness for most hydrological models which may be related to an underlying assumption used in developing the model. For instance, Adera and Alfredsen [16]; Abdulahi et al. [25], and Heyi and Dinka [29]stated that the HVB model caused a significant difference between the simulated and observed upper extreme values and the model had better performed in predicting the medium-range flow. According to Kannan [55] and Halwatura and Najim [56], the effectiveness of the SCS-CN method was experimentally tested in a small agricultural watershed in the mid-western United States. In addition, the method neglects the effect of rainfall duration and intensity on surface runoff generation. Therefore, applying the method directly may result in a significant error, particularly for the upper extreme flows. On the other hand, Kannan [55] proved that the SCS-CN method still outperforms the Green and Ampt in predicting the peak flow.
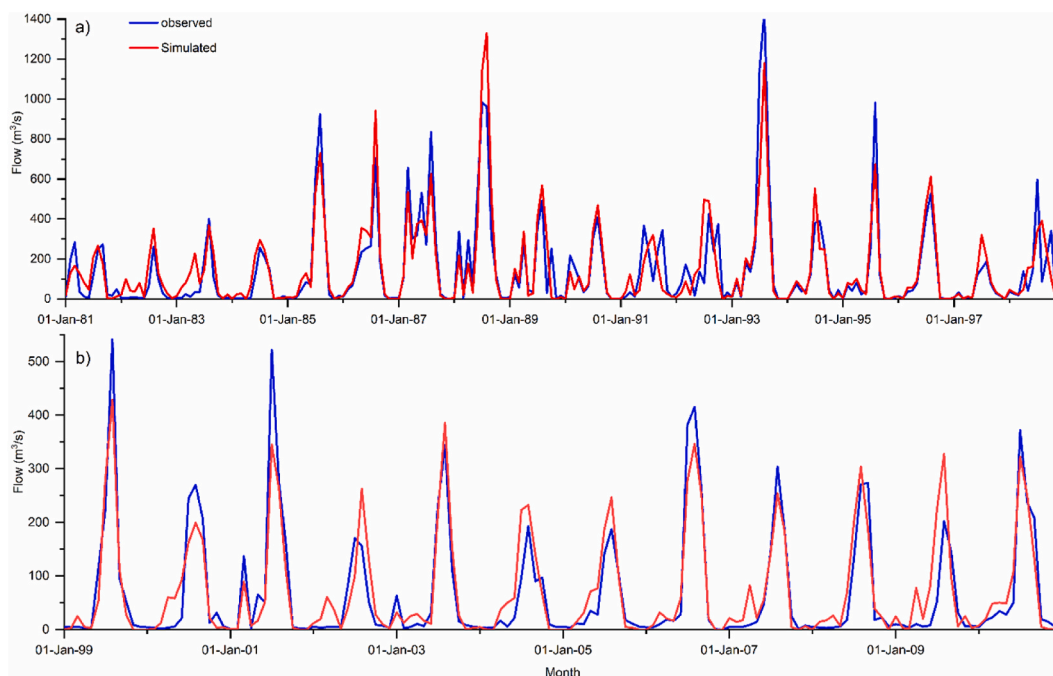

Fig. 4. Monthly simulated and observed hydrographs of the Upper Awash watershed for the calibration (a) and validation (b) periods.

3.2. Analysis of the monthly inflow of koka reservoir

The monthly inflow into the Koka reservoir was simulated throughout the study period using the calibrated and validated SWAT model. According to the study, the simulated monthly inflow to Koka reservoir showed upward trend. The result shows that the inflow into the reservoir in the 2020s under the RCP4.5 scenario is projected to decrease by −28.707% compared to the simulated inflow during the reference period. However, the monthly inflow to Koka reservoir could increase by 4.635% under the RCP8.5 scenario. In the 2050s and 2080s the mean annual monthly inflow to the reservoir will likely increase by +5.672% (+5.764%) and +4.011% (+10.470%) under the RCP4.5 and RCP8.5 scenarios, respectively. The maximum increment will likely to occur during the 2080s under the RCP8.5 scenario. The result indicates that the Koka reservoir inflow is projected to increase in the 2050s and 2080s compared to the inflow of the reference period. This conclusion is consistent with those made by Adera and Alfredsen [16]; Dibaba et al. [19] and Abdulahi et al. [25]. During the reference period, the annual average inflow of Koka reservoir was 139.675 MCM. However, the inflow analysis under the two scenarios from 2011 to 2100 showed that the minimum annual inflow was 99.578 MCM during the 2020s, and the maximum annual inflow was 156.008 MCM during the 2080s under the RCP8.5 scenario. Hence, the simulated inflow under the RCP4.5 scenario showed a diminishing signal. The result also showed that the temporal variability of inflow of the Koka reservoir variability will most likely decrease in future periods. The maximum standard deviation of the inflow, as shown in Table 5, was during the reference period (164.669 MCM). On the other hand, the inflow fluctuation was less in the 2020s and 2050s periods.

Fig. 5 shows the 30-year average inflow of Koka reservoir during the reference, the 2020s, 2050s, and 2080s periods. The graph indicates that the highest monthly inflow will likely occur from June through November. Hence, during the reference period, the June–November inflow was higher than the monthly inflow during 2020s, 2050s and 2080s. Accordingly, the maximum inflow to the Koka reservoir was 519.767MCM, which was computed during the reference period in August. Ethiopia experiences its wettest season from June to November. The analysis of the observed rainfall data indicated that maximum rainfall was observed in August. Consequently, the monthly distribution of inflow follows the seasonal dynamics and pattern of rainfall. The inflow from December to May, which belongs to the winter and autumn season of Ethiopia, was minimum throughout the study period. Fig. 5 shows that compared to the inflow of the reference period, the magnitude and temporal dynamics of the inflow in the 2020s, 2050s, and 2080s are similar. Therefore, considering the magnitude and pattern of the inflow, the effect of climate change on the inflow to the Koka reservoir is optimistic. This doesn't entirely imply that there is no negative impact on the inflow to the reservoir. For instance, during the reference period, the inflow into the Koka reservoir from January to August was higher than the inflow of the reservoir in the 2020s, 2050s, and 2080s. On the other hand, the average monthly observed inflow was less than the inflow predicted by the output of the climate model from August to September during the reference period. With the exception of the inflow during the 2020s under the RCP4.5 scenario, the peak inflow has shifted from August during the reference period to September during the 2020s, 2050s, and 2080s periods. The result is also consistent with the findings of Abera et al. [10]; Adera and Alfredsen [16], and Leta et al. [52]. Therefore, climate change on the Koka reservoir will most likely increases the magnitude of the inflow and shift its temporal distribution.

The impact of climate change is also different on different flow ranges. In order to select and implement local specific water resource management scenarios for a particular flow type, it is crucial to quantify the rate of change and signal of climate change at different flow regimes. Accordingly, the relative change and signal of flow due to climate change at different flow range was investigated using flow duration curve. To quantify the impact of climate change on different flow regimes, the flow was divided into various flow regimes using the probability of exceedance, which can be computed from the flow frequency. Emiru et al. [22] studied the impact of climate change on Upper Awash stream flow at low flow (Q90) and high flow (Q5). Accordingly, it is not ambiguous to identify the low flow and high flow from the flow duration curve. However, detail flow classification helps to ensure a smooth transition across different flow categories. The classification of flow between the upper and lower flow range is slightly different by different scholars. In this study, the widely known and accepted classification adopted by Kwakye [57] was used to classify the flow of the Upper Awash watershed into high flow (Q0-Q9.722), wet condition (Q10-Q39.722), mid-range flow (Q40-Q59.722), dry period condition (Q60-Q89.722), and low flow (Q90-Q100) based on their exceedance probability.

According to the analysis, the mean annual flow for the reference period with a 0–10% probability of exceedance was equalled or exceeded 225.724 m^3/s. However, a constant decrease was confirmed by the high flow in the 2020s, 2050s, and 2080s. Hence, the high flow in the future revealed a negative signal. Under the RCP8.5 scenario, the maximum and minimum relative changes were −28.528% and −22.856% with respect to the reference period's high flow, respectively. These changes are likely to occur in the 2020s and 2050s.

In contrast to the high flow, the wet condition, the mid-range, dry period condition, and the low flow showed a constant increasing

Table 5
Monthly inflow to the Koka reservoir throughout the study period.

| Study period	Mean (MCM)	Standard Deviation (MCM)	Minimum (MCM)	Maximum (MCM)
Reference (1981–2010)	139.675	164.669	6.013	519.767
RCP4.5 (2011–2040)	99.578	115.070	3.910	367.727
RCP8.5 (2011–2040)	146.463	149.075	2.497	406.285
RCP4.5 (2041–2070)	148.073	149.224	2.608	392.381
RCP8.5 (2041–2070)	148.219	148.562	2.717	388.934
RCP4.5 (2071–2100)	145.512	146.147	3.546	386.893
RCP8.5 (2071–2100)	156.008	159.566	4.966	422.218
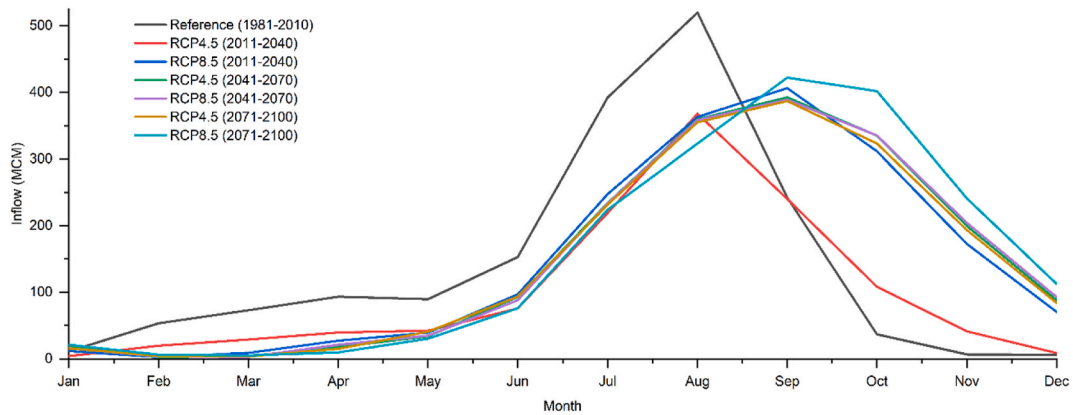
Fig. 5. Monthly average inflow of the Koka reservoir (1981–2100).

signal throughout the study period. However, aside from the low flow, every flow category in the 2020s under the RCP4.5 scenario showed a negative signal. This can be because of many uncertainties associated with assumptions made in the scenario, inadequate conceptualization of the climate and hydrological model, and uncertainty related to the physical properties of the watershed. However, the relative change and signal that the RCP8.5 scenario comply with are more consistent throughout the entire study period. As a result, the outlier of the flow signal and the relative change caused by the RCP4.5 scenario have no impact on the finding of this study.

The increase in low flow over subsequent periods is the most encouraging result of the study. During the reference period, the average value of high flow with an exceedance probability of 0–10% was 0.033 m^3/s. However, the relative change of the average low flow values during the 2020s, 2050s, and 2080s were, +80.098% (+89.510%), +82.138% (+78.407%), and +90.401% (+89.617%) under the RCP4.5 and RCP8.5 scenarios, respectively compared to their corresponding values during the reference period. The maximum future low flows that equalled or exceeded 0–10% of the time were 0.344 m^3/s and 0.318 m^3/s were also under the two forcing scenarios respectively.
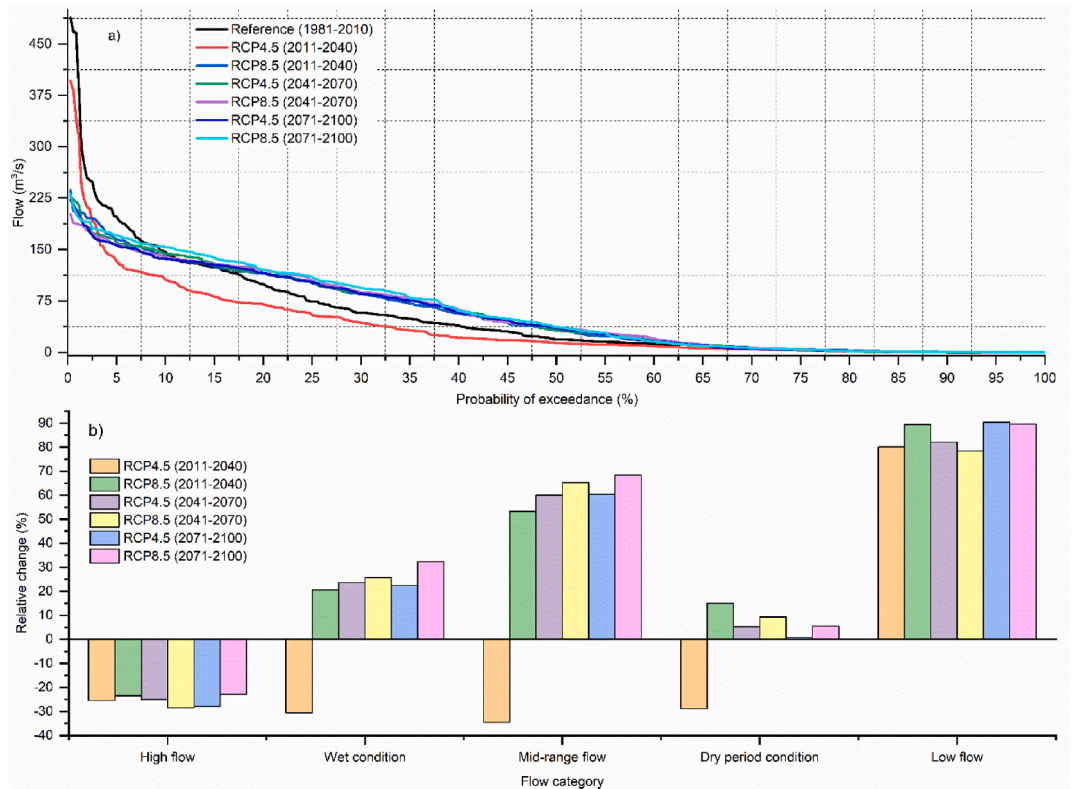

Fig. 6. Flow duration curve (a) and the relative change of flow at different flow regimes of the Koka reservoir (b).

Out of all the flow regimes, the relative increase in low flow is the one with the highest likely increment for the future period. Thus, the study has proved that the main impact of climate change is to shift the high flow into low flow. Consequently, the high flow is predicted to decrease under the influence of climate change. Conversely, the low flow is expected to increase. Furthermore, the inter-annual and monthly inflow showed little fluctuation due to the increasing signal of low flow. Based on the finding, the standard deviation of the monthly inflow during the 2080s was less than that of the reference period. This signifies that there will be less variation in inflow during the future periods than the inflow during the reference period.

Quantifying the impact of climate change on the inflow at different flow categories is used to modify the reservoir rule curve. In order to maximize the frequency of reservoir rule curve, little inflow variation is crucial. This helps to reduce the level of uncertainty in reservoir operation. Fig. 6 (a) revealed that the high flow during the reference period was lower than the flow with an exceedance probability of 0–9.722%. Nevertheless, the flow with a 10–100% exceedance probability exhibited a rising signal.

3.3. Analysis of the monthly optimal elevation of koka reservoir

The monthly optimum elevation was computed by HEC-ResPRM using the monthly inflow, storage penalty functions, elevation, storage, and outflow constraints as input to the model. In this study, the average deviation of the observed storage against the target storage was used to develop a penalty function. During the initial stage of reservoir operation, the target inactive storage was 180 MCM. However, the ten-year monthly average observed storage was 250 MCM, which is a 28% deviation from the target minimum operating storage. Consequently, the penalty assigned at 180 MCM was 28. The active storage capacity of the Koka reservoir was 1680 MCM. On the other hand, the average ten-year observed storage capacity analysis revealed that the actual active storage capacity was 1206.860 MCM, depicting a deviation of 28.163% from the target storage capacity. Similarly, the total storage capacity is 1850 MCM. However, the observed average storage capacity deviated from the target storage capacity of Koka reservoir by 36.757%. Table 6 shows the penalty values assigned at each storage level.

Table 6 shows the increment of penalty with elevation/storage. The cost of deviation from the desired system operation of the Koka reservoir is represented by this pricewise linear penalty function. In HEC-ResPRM, network flow programming minimizes unit cost by distributing the inflow into the arc with the minimum slope penalty function. As a result, the solution to optimum storage, elevation, release, and power capacity is the minimum slope of the penalty function established on the Koka reservoir's arc, which is found between the inflow and outflow nodes of the reservoir.

Based on the result, the minimum, maximum, and mean monthly optimal elevation values of the Koka reservoir during the reference period were 1581.900 m, 1593.200 m, and 1590.771 m (a.m.s.l), respectively. The result indicates that the Koka reservoir was operated at maximum elevation during the reference period. However, the optimal elevation of the Koka reservoir will likely decrease compared to its correspondence value during the reference period due to the impact of climate change. Accordingly, the mean monthly elevation will likely decrease by (0.618 m) (0.343 m), 0.348 m (0.440 m), and 0.256 m (0.276 m) under the RCP4.5 and RCP8.5 scenarios in the 2020s, 2050s, and 2080s, respectively. As shown in Table 7, the mean, minimum, and maximum elevations of the Koka reservoir were 1590.423 m, 1581.30 m, and 1593.20 m a.m.s.l, respectively, under the RCP4.5 scenario from 2041 to 2070. The result also showed that the reservoir might be operated at the lowest elevation during the 2050s under the RCP4.5 scenario.

In order to investigate the optimizing ability of the HEC- ResPRM, the optimum monthly elevation was compared to the actually operated elevation from 2011 to 2021. Statistically, the mean, minimum, and maximum observed elevations of Koka reservoir were 1587.541 m, 1583.514 m, and 1591.087 m a.m.s.l, respectively. These values are the lowest throughout the study period compared to the optimized elevation. Hence, the analysis revealed that the Koka reservoir was not optimally operating during the reference period. This indicates that the operation of the reservoir at lower elevation is not due to lack of inflow into the reservoir because the optimized

Table 6
Elevation/storage penalty value of Koka reservoir.

Elevation (m)	Target Storage (MCM)	Actual Storage (MCM)	Penalty (%)
1580.400	180	250.000	28.000
1589.950	1680	1206.860	28.163
1590.700	1850	1170.000	36.757

Table 7
Monthly average optimum elevation[a] of the Koka reservoir during the study period.

Operation period	Mean (m)	Minimum (m)	Maximum (m)
Reference (1981–2010)	1590.771	1581.900	1593.200
Observed (2011–2021)	1587.541	1583.514	1591.087
RCP4.5 (2011–2040)	1590.153	1581.800	1593.200
RCP8.5 (2011–2040)	1590.428	1581.700	1593.200
RCP4.5 (2041–2070)	1590.423	1581.300	1593.200
RCP8.5 (2041–2070)	1590.331	1581.700	1593.200
RCP4.5 (2071–2100)	1590.515	1581.700	1593.200
RCP8.5 (2071–2100)	1590.495	1581.300	1593.200

[a] Mean sea level is taken as a reference level to express the optimum elevation of Koka reservoir.

elevation is higher than the observed elevation during the same study period.

As shown in Fig. 7, the magnitude and temporal distribution of optimum elevations under the RCP4.5 and 8.5 scenarios are similar and the two graphs are close to each other. This indicates that the impact of climate change on the operating level of the Koka reservoir is adequately represented by the HEC-ResPRM model. However, throughout the study period, the minimum operating level of the reservoir was higher than that of the dead storage level. The study also revealed that the optimum monthly elevation increased from the reference to the end-of the century (2080s) under the two RCP scenarios. As illustrated in Fig. 7 (b), the actual operating level of the Koka reservoir was mainly lower than the optimum reservoir level. Even during the rainy season of Ethiopia, the reservoir was not full. Therefore, the additional optimum storage level obtained in this study can be used to store more water, reducing the risk of water scarcity during the dry season and producing more power. Furthermore, because the reservoir has more space to store excess water without overflowing, the risk of flooding can be reduced during periods of high flood.

Fig. 7 also shows that the elevation rapidly increases from 1981 to 1983 during the reference period. However, the rate of increment is expected to decrease between 1984 and 2100. The network flow programming distributes more water to the minimum penalty value because the minimum storage penalty was assigned at the dead storage level. As a result, the optimum elevation increment was from the dead storage level to the normal pool level of the reservoir. If the model does not achieve optimum elevation, the initially assigned penalty values can be slightly modified to obtain the optimal elevation and storage of the reservoir. However, in this study, the optimum reservoir level was determined by the initial values of storage penalty functions and outflow constraints.

The release from the reservoir for environmental and irrigation purposes is less than the inflow of the reservoir. Consequently, the new incoming flow will be added to the previously stored water. Due to this, the elevation showed a continuous increasing signal. However, even though the optimum elevation increased, it cannot extend beyond the maximum flood level of the dam which is 1593.20 m a.m.s.l. Hence, the optimum elevation corresponds to the flood level of the Koka reservoir. Accordingly, the additional elevation of the reservoir will be 2.5 m. As shown in Fig. 7, the minimum and maximum storage levels fluctuate around the optimum operating level of the reservoir. This indicates that the reservoir can quickly recover if its level is dropped to the minimum level for power production.

Fig. 8 shows the 30-year monthly average elevation during the reference, 2020s, 2050s, and 2080s periods. The result indicates that the long-term monthly optimum elevation was also maximum during the reference period (1592.210 m a.m.s.l.). Furthermore, the analysis of monthly inflows into the Koka reservoir revealed that the reference period had the highest average inflow. On the other hand, the monthly average elevation during the 2020s, 2050s, and 2080s shows a similar pattern with little elevation difference between the specified time periods.

The graph (Fig. 8) also indicates that the average elevation is likely to decrease during the dry months. Hence, the minimum operating level of Koka reservoir was computed in June, which is the transition month from the autumn to the summer in Ethiopia. According to the analysis, the optimum elevation values of the Koka reservoir during August, September, October, and November were 1591.683 m, 1592.210 m, 1591.880 m, and 1591.870 m, respectively. March, April, May, and June showed the lowest elevation values (1590.047 m, 1589.970 m, 1589.810 m, and 1589.867 m a.m.s.l., respectively). The result is also supported by Sharaky et al. [7] and Abera et al. [10].

3.4. Analysis of the monthly optimum storage capacity of the koka reservoir

The monthly inflow of Koka reservoir simulated by SWAT model was used to compute the monthly power capacity. Therefore, the average storage volume represents the useable storage capacity in this study. However, the actual minimum and maximum storage may be affected by the maximum inactive storage level, peak demand, and electromechanical equipment efficiency. At normal operating levels, the maximum storage capacity of the Koka reservoir is 1850 MCM. The HEC-ResPRM requires the user to provide a minimum and maximum storage capacity, which can be used as a boundary value to simulate the optimum storage capacity. Therefore, the actual maximum and minimum storage capacity of the Koka reservoir was directly used as a lower and higher boundary values during the initial optimization phase. However, the solution for network flow programming in HEC-ResPRM, was not feasible. Because the inflow into the reservoir exceeded the carrying capacity of the reservoir. As a result, during the subsequent optimization phases, the initial lower and higher boundary values were 180 MCM and 2500 MCM, respectively. However, the model simulated the final optimum value of storage by taking into account the storage penalties, constraints, and inflow capacity.

According to the analysis, the average monthly observed storage was 1207 MCM. However, the average monthly optimum storage during the reference period was higher than that of the observed storage by 35.136%. Similarly, the optimized storage capacity during the 2020s, 2050s, and 280s study periods showed a relative increment of +30.875% (+32.903%), +32.797% (+32.123%), and +33.297% (+33.352%) under the RCP4.5 and RCP8.5 scenarios, respectively as compared to the observed storage.

On the other hand, the Koka reservoir has a designed useable storage capacity of 1680 MCM. However, during the reference period, the optimum storage increased by +9.717% compared to the designed useable storage capacity. Similarly, the designed useable storage capacity increased by +3.787% (+6.609%), +6.461% (+5.523%), and +7.158% (7.234%) during the 2020s, 2050s, and 2080s study periods under the RCP4.5 and RCP8.5 scenarios, respectively. The results showed that useable storage capacity increased the most during the reference period compared to the observed and useable storage capacity throughout the study period. The monthly distribution of optimum storage capacity is similar to the monthly distribution of optimum elevation of the Koka reservoir. The overall minimum average storage for the entire study period was 1542.550 MCM, which was obtained in July. This is because July is the beginning month for reservoir filling. As a result, the monthly average inflow of the Koka reservoir for the entire study period indicates that maximum inflow occurs from July to October (Fig. 9).

Fig. 10 depicts a box plot of the average storage capacity for the reference, the 2020s, 2050s, and 2080s periods. The graph also
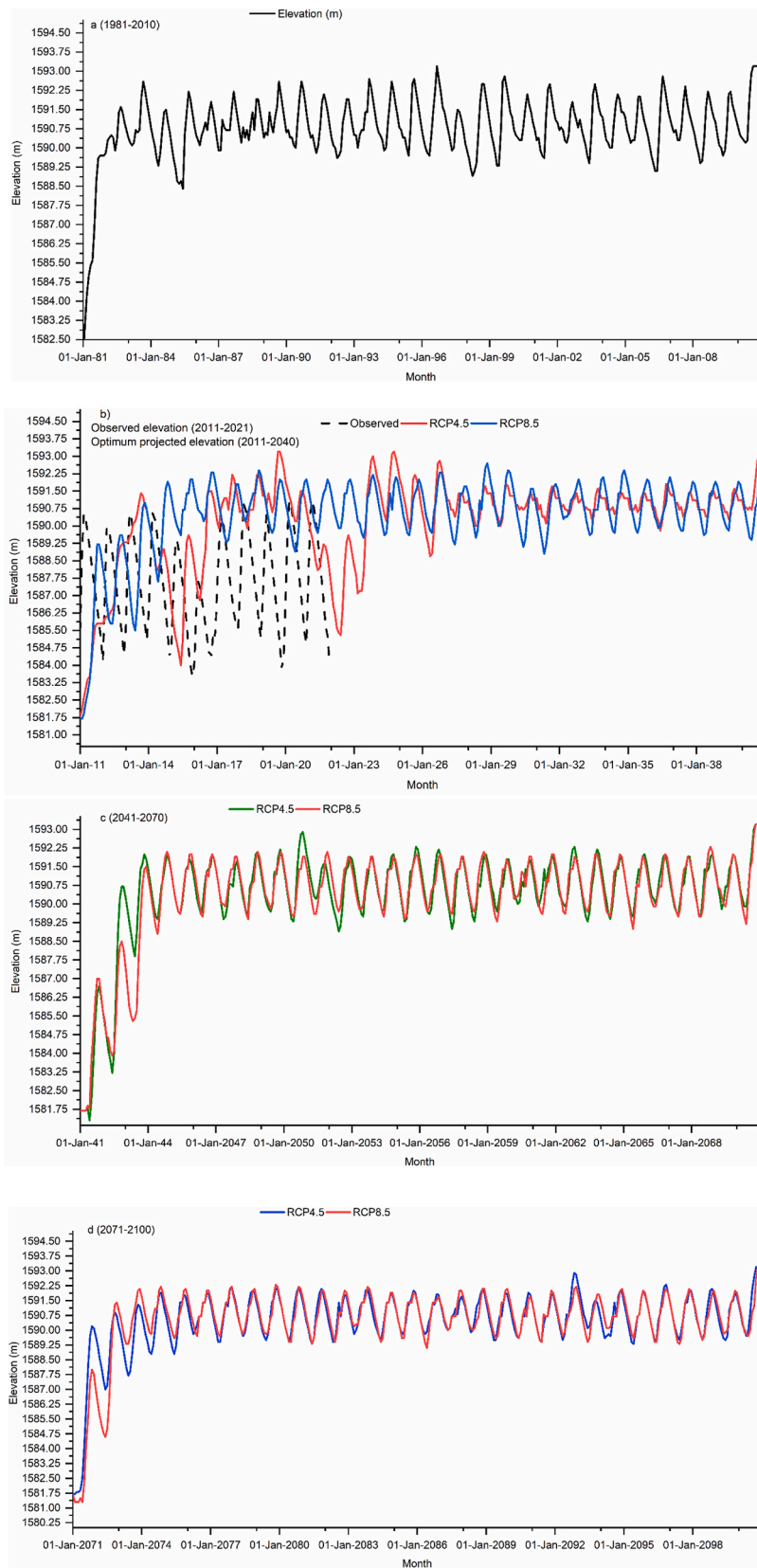
Fig. 7. The monthly optimum elevation of Koka reservoir for the reference (a), the 2020s (b), 2050s (c) and 2080s (d) periods.
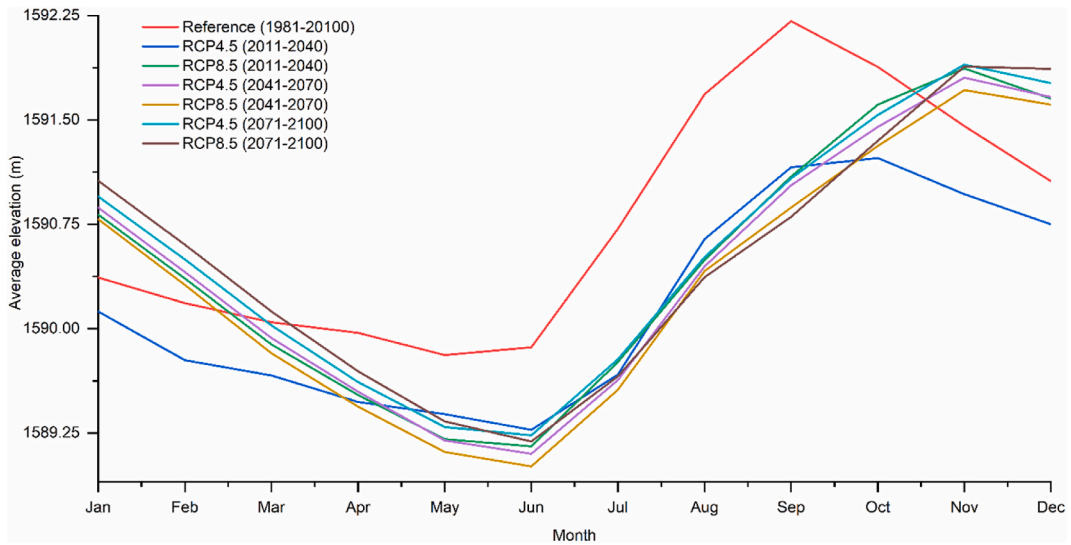
Fig. 8. The mean monthly elevation of the Koka reservoir (a.m.s.l) under the reference, 2020s, 2050s, and 2080s periods.
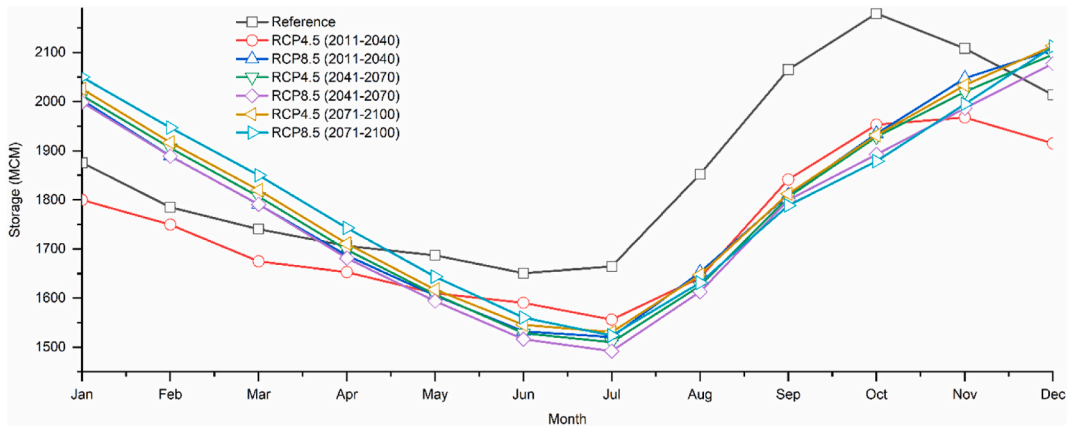

Fig. 9. The Monthly average optimum storage capacity of the Koka reservoir.
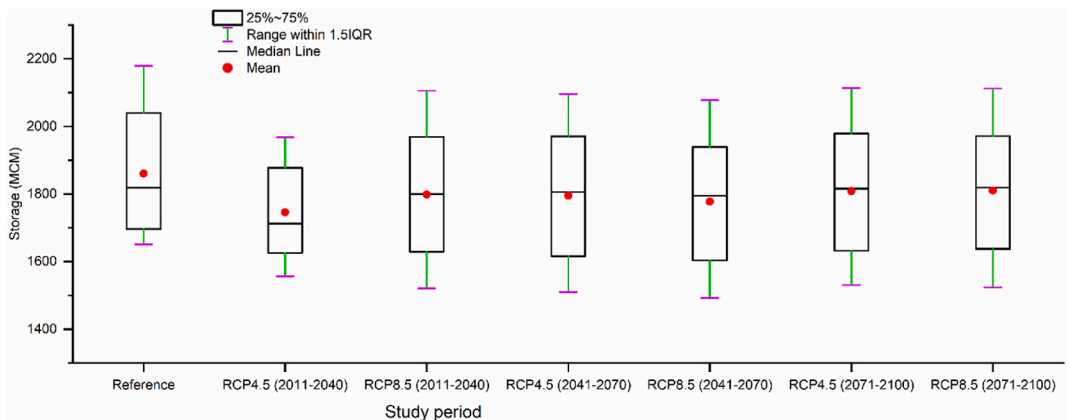

Fig. 10. Box plot of the relative change in optimum storage capacity of the Koka reservoir.

demonstrated that the maximum storage capacity was obtained during the reference period. However, storage capacity is expected to decline during the 2020s, 2050s, and 2080s periods compared to the storage capacity during the reference period. According to the analysis, the maximum and minimum declining rates were −6.164% and −2.677%, respectively, during the 2020s under the RCP4.5 and the 2080s under the RCP8.5 scenario.

3.5. Analysis of the monthly optimum power capacity of koka reservoir

The average optimum monthly power capacity throughout the reference period was 16.489 MW. The monthly observed average power, on the other hand, was 11.224 MW. The findings revealed that the Koka reservoir was not being operated optimally during the reference period. Lack of efficient management of the Koka reservoir is one possible explanation for the reservoir operating below its optimum capacity. For example, rapid water release during the summer season with a danger of flood inundation downstream of the Koka hydropower plant. The reservoir was designed to hold more water during the summer and operate during the other seasons. However, rapid water release to the downstream of the reservoir results in the release of energy without any use. As a result, the stationary assumption of hydro meteorological variables, which leads to reservoir to be operated based on the past rule curve, has reduced the optimal operation of the Koka reservoir.

The optimum power capacity throughout the 2020s, 2050s, and 280s periods increased by +31.280% (+31.281%), +32.066% (+32.069%), and +32.025%, (+32.193%) under the RCP4.5 and RCP8.5 scenarios, respectively, as compared to the observed power. As a result, the optimum power capacity of the Koka reservoir under climate change will likely be more than the actual produced power. Similarly, optimum power capacity is expected to rise in the 2020s, 2050s, and 2080s periods compared to their respective value during the reference period. Under RCP4.5 and RCP8.5 scenarios, the relative changes throughout the 2020s, 2050s, and 2080s periods compared to the reference period were −0.948% (+0.161%), +0.199% (+0.202%), and +0.138% (+0.386%). The overall result showed that optimum power capacity is projected to increase due to climate change.

The analysis also showed that the maximum and minimum monthly observed power were 13.779 MW and 9.736 MW, respectively. The discrepancy between the maximum and minimum values indicated the existence of high-power fluctuation during the observed period. However, the difference in the optimized monthly power capacity for the reference, 2020s, 2050s, and 2080s, as shown in Table 8, verified the likely existence of little fluctuation throughout the whole study period. The reason could be concomitant to the increment of low flow and the decrement of high flow which possibly shifted to increase the mid-range flow.

The monthly distribution of produced power revealed that maximum power was produced during the driest season in Ethiopia. Based on the analysis, the observed values of power during February, March, and January were11.391 MW, 13.779 MW, and 13.477 MW, respectively. This indicates that maximum release was during the dry months, and the reservoir was allowed to store more water during the wettest season. As shown in Fig. 11, the monthly power attains its peak value during February and continually decreased afterwards. However, the optimized power proved that the power capacity was maximum from February to August during the reference period following the pattern of inflow. On the contrary, the optimum power during the reference period from September to December attained its minimum value compared to the optimum power capacity during the 2020s, 2050s, and 2080s study periods.

Based on the finding, the maximum power capacity values throughout the study period were 17.387 MW, 17.297 MW, and 16.960 MW, which were obtained during August, September, and October, respectively. The maximum power capacity during the reference period was 17.915 MW, which was mimicked in August, whereas the peak power capacity values during the 2020s, 2050s, and 2080s were 17.325 MW (17.481 MW), 17.457 MW (17.421 MW), and 17.436 MW (17.560 MW), respectively, under the RCP4.5 and RCP8.5 scenarios, which were obtained in September. The analysis indicates that climate change is also responsible for the shift in peak values of the power capacity from August to September.

During the observed period, the produced power showed subsequent decline even during the wet season. However, if the reservoir is optimally operated, there will be a chance of refilling the reservoir for the subsequent year. Because the inflow during the wet season is abundant, allowing the reservoir to hold water above its normal operating level. As a result, it is possible to generate power while also storing water.

According to Hamududu and Killingtveit [6], the power capacity in East Africa showed a general rising trend under the impact of climate change. However, if the existing reservoir operation rule is not modified, the optimum power capacity cannot be fully utilized. Therefore, the study proposed reservoir filling and operation alternatives based on inflow variation. In this study, the optimum power capacity was obtained during the wettest season of Ethiopia. As a result, there are two options to operate the Koka reservoir. The first is filling the reservoir to its maximum capacity, which is simulated in this study and operates at full capacity during the dry seasons.

Table 8
Statistical summary of optimized power capacity and actually produced power.

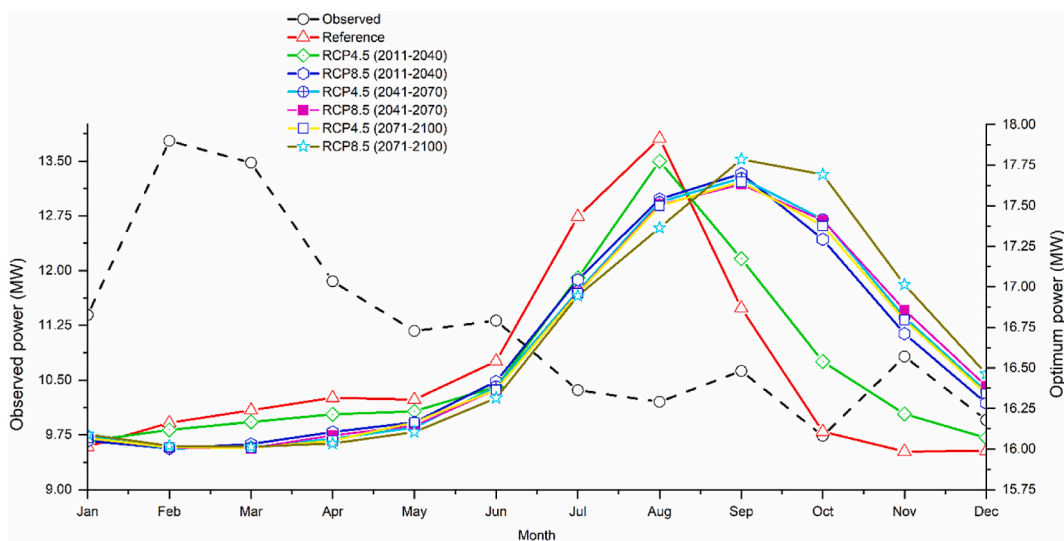| Study period	Mean (MW)	Maximum (MW)	Minimum (MW)
Observed	11.224	13.779	9.736
Reference	16.489	17.915	15.985
RCP4.5 (2011–2040)	16.333	17.325	15.983
RCP 8.5 (2011–2040)	16.516	17.481	15.975
RCP4.5 (2041–2070)	16.522	17.457	15.975
RCP8.5 (2041–2070)	16.522	17.421	15.976
RCP4.5 (2071–2100)	16.512	17.436	15.979
RCP8.5 (2071–2100)	16.553	17.560	15.985

Fig. 11. The monthly optimum power during the reference (a), 2020s (b), 2050s (c), and 2080s (d).

Hence, rather than shifting the operational season, the existing operation rule should be modified to account the effects of climate change. Thus, operating the reservoir more during the dry months and less during the wet months can helps in storing water for the dry months. The irrigation and environmental water requirements, on the other hand, typically becomes maximum during the dry season. As a result, the second option is reservoir filling and power generation should be a simultaneous activity that can align with the temporal dynamics of the inflow. However, due to limited storage, the power production capacity should be enhanced during the rainy season by directly feeding the incoming excess flood to the turbine.

Fig. 12 (a) shows that there was during the reference period. However, the monthly power distribution under the two scenarios will likely become uniform and consistent. The monthly observed power distribution is also shown on the graph to demonstrate how the observed power distribution behaves with the optimum power capacity mimicked by the HEC-ResPRM (Fig. 12 (b)).

3.6. Limitations of the study

In this study, the projected climate change is based on the RCP4.5 and RCP8.5 scenarios, which are developed based on emission, concentration, and land use trajectories that result in varying levels of radioactive forcing. Detail understanding of the future LU/LC trajectory, greenhouse and aerosol emissions, and the conversion of those gases into climate change may lead to a better understanding of the trend of radio-active forcing. Therefore, the uncertainty of future population growth, socioeconomic activities, changes in living standards, and new technological development may influence the spatiotemporal variation of LU/LC, as well as the emission and concentration of greenhouse gases. As a result, new updated scenarios could be developed. On the other hand, no scenario can be developed in the absence of uncertainty. Internal variability in climate change may also cause uncertainty. As a result, the projected climate may deviate from the RCP4.5 and/or RCP8.5 scenarios. Therefore, this study indicates the likely impact of climate change, which may not accurately represent the actual inflow, storage, elevation and power capacity of Koka reservoir during the respective future study periods.

4. Summary and conclusions

In this study, the impact of climate change on the inflow and optimal operation of the Koka reservoir was investigated from 1981 to 2100. During the reference period, the observed climate data were used to simulate the monthly inflow, optimum elevation, storage, and hydropower capacity of Koka reservoir, whereas from 2011 to 2100, the climate data from the multimodal ensemble of DMI-HIRHAM5, KNMI-RACMO22T, CLMcom-CCLM4-8-17, RCA4, REMO2009, and CanRCM4 under the RCP4.5 and RCP8.5 scenarios were used to forecast the monthly inflow of Koka reservoir using the SWAT model. Even though the future climate pattern may not follow the RCP8.5 and 4.5 scenarios, the monthly pattern of the projected values of inflow, elevation, storage, and hydropower capacity agrees with their corresponding observed values from 2011 to 2021. The SWAT model was calibrated from 1981 to 1998 and validated from 1999 to 2010 using the monthly observed stream flow near the outlet of Upper Awash watershed. The graphical and statistical analysis of the simulated and observed runoff hydrographs during the calibration and the validation periods indicated that the SWAT model is suitable and adequate for the monthly surface runoff simulation of the Upper Awash watershed. Based on the result, the monthly inflow into the Koka reservoir is expected to rise due to climate change. During the reference period, there was a significant inter-annual inflow variation. However, the variation of inflow from 2011 to 2100 is not significant, which is a favorable feature of climate change for the Koka reservoir. However, as a result of climate change, the occurrence month of the highest inflow of
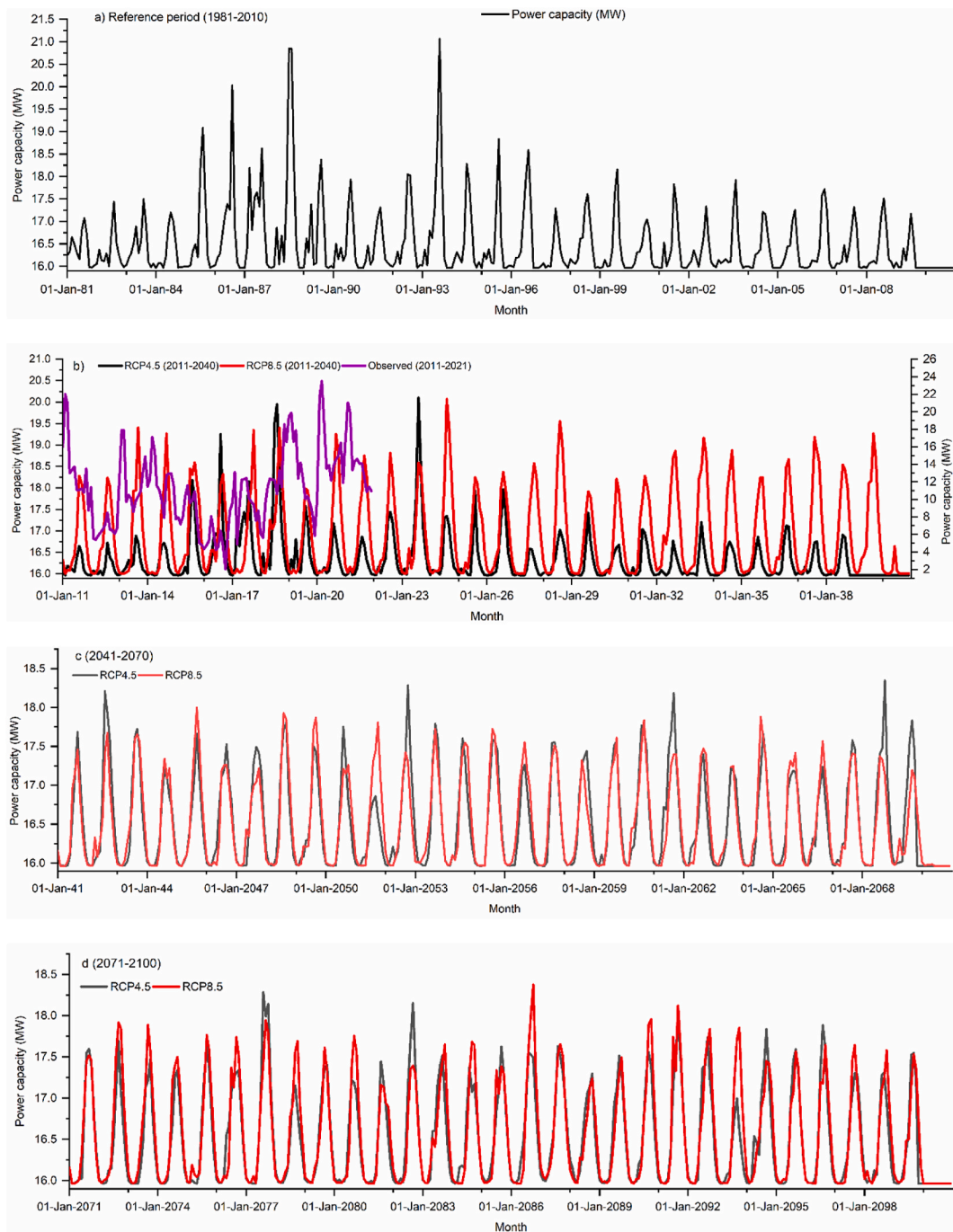
Fig. 12. Monthly distribution of optimized and observed power.

the Koka reservoir will likely shift from August to (September–October). The influence of climate change was also studied using different flow regimes of the Upper Awash watershed. The results showed that high flow shows a diminishing signal, but the wet, mid-range, and dry period, and low flow show a steady increasing signal throughout the study period. Therefore, the novel finding of the study is that there is a shift in the monthly occurrence of peak discharge, increment of low flow, and decrement of high flow due to climate change.

The other novel finding of the study is the use of penalty functions and physical constraints of the Koka reservoir to bring the system to the desired operation in HEC-ResPRM. Following the inflow pattern, the optimum elevation and storage showed a slightly increasing. Compared to the observed storage and elevation, the values of optimum elevation and storage was the highest throughout the study period. However, during the reference period, the values of optimum elevation and storage were higher than their

corresponding values in the 202s, 2050s, and 2080s. This study also indicated that the power capacity of the Koka reservoir will likely increase under the impact of climate change. Based on the analysis, the optimized power capacity is higher than the observed power of the Koka reservoir. However, following the seasonal shift of the inflow, there is also a shift in the monthly distribution of hydropower capacity. Accordingly, the occurrence month of the peak hydropower capacity will likely shift from August to (September–October). The study indicated that the inflow, storage, elevation and power capacity will likely increase under the impact of climate change. Accordingly, the operation of the Koka reservoir should consider the likely impact of climate change. Accordingly, the existing reservoir rule curve should be modified to utilize the additional power capacity of the Koka reservoir. The long-term average elevation, storage, and hydropower capacity obtained in this study can be used as a rule curve under the uncertainty due to climate change. The study is also important to analyze the difference between the past and the present operation and the likely operation of the Koka reservoir in the future time horizon. In this regard, the study is vital to develop feedback mechanisms for efficient and optimal power generation. However, this study does not consider the temporal variation of LU/LC and demand change associated with the socio-economic activity of the population. Therefore, further study should be conducted to address the impact of LU/LC and demand change on the operation of the Koka reservoir. The future study should also consider a recently updated scenarios and climate models to assess the impact of climate change on the available water resources and hydropower capacity of the watershed.

Author contribution statement

Sewmehon Sisay Fanta: Mamuye Busier Yesuf: Tamene Adugna Demissie: Conceived and designed the experiments; Performed the experiments; Analyzed and interpreted the data; Contributed reagents, materials, analysis tools or data; Wrote the paper.

Data availability statement

Data will be made available on request.

Declaration of competing interest

The authors declare that they have no known competing financial interests or personal relationships that could have appeared to influence the work reported in this paper.

References

[1] Y. Seleshi, U. Zanke, Recent changes in rainfall and rainy days in Ethiopia, Int. J. Climatol. 24 (8) (2004) 973–983, https://doi.org/10.1002/joc.1052.
[2] G. Kebede, W. Bewket, Variations in rainfall and extreme event indices in the wettest part of Ethiopia, Sinet: Ethiop. J. Sci 32 (2) (2009) 192, https://doi.org/10.4314/sinet.v32i2.68864, 140.
[3] H.O. Misiani, D.L. Finney, Z.T. Segele, J.H. Marsham, A. Tadege, G. Artan, Z. Atheru, Circulation patterns associated with current and future rainfall over Ethiopia and South Sudan from a convection-permitting model, Atmosphere 11 (12) (2020) 1352, https://doi.org/10.3390/atmos11121352.
[4] T.B. Tariku, K.E. Gan, X. Tan, T.Y. Gan, H. Shi, A. Tilmant, Global warming impact to River Basin of Blue Nile and the optimum operation of its multi-reservoir system for hydropower production and irrigation, Sci. Total Environ. 767 (2021), 144863, https://doi.org/10.1016/j.scitotenv.2020.144863.
[5] S.E. Chaemiso, A. Abebe, S.M. Pingale, Assessment of the impact of climate change on surface hydrological processes using SWAT: a case study of Omo-Gibe River basin, Ethiopia, Model. Earth Syst. Environ. 2 (4) (2016) 1–15, https://doi.org/10.1007/s40808-016-0257-9.
[6] B. Hamududu, A. Killingtveit, Assessing climate change impacts on global hydropower, Energies 5 (2) (2012) 305–322, https://doi.org/10.3390/en5020305.
[7] A.M. Sharaky, K.H. Hamed, A.B. Mohamed, Model-based optimization for operating the Ethiopian renaissance dam on the blue nile river, Handb. Environ. Chem, spriger, cham 79 (2017) 119–148, https://doi.org/10.1007/698_2017_188.
[8] D. Jaweso, B. Abate, A. Bauwe, B. Lennartz, Hydro-meteorological trends in the upper Omo-Ghibe river basin, Ethiopia, Water (Switzerland) 11 (9) (2019) 1951, https://doi.org/10.3390/w11091951.
[9] J.L. Fan, J.W. Hu, X. Zhang, L.S. Kong, F. Li, Z. Mi, Impacts of climate change on hydropower generation in China, Comput. Simulat. 1670 (2018) 4–18, https://doi.org/10.1016/j.matcom.2018.01.002.
[10] F.F. Abera, D.H. Asfaw, A.N. Engida, A.M. Melesse, Optimal operation of hydropower reservoirs under climate change: the case of Tekeze reservoir, Eastern Nile, Water 10 (3) (2018) 273, https://doi.org/10.3390/w10030273.
[11] D. Raje, P.P. Mujumdar, Reservoir performance under uncertainty in hydrologic impacts of climate change, Adv. Water Resour. 33 (3) (2009) 312–326, https://doi.org/10.1016/j.advwatres.2009.12.008.
[12] D. Prasanchum, A. Kangrang, Optimal reservoir rule curves under climatic and land use changes for Lampao Dam using Genetic Algorithm, KSCE J. Civ. Eng. 22 (2018) 351–364, https://doi.org/10.1007/s12205-017-0676-9.
[13] V. Nourani, N. Rouzegari, A. Molajou, A.H. Baghanam, An integrated simulation-optimization framework to optimize the reservoir operation adapted to climate change scenarios, J. Hydrol. 587 (2020), 125018, https://doi.org/10.1016/j.jhydrol.2020.125018.
[14] B.A. Faber, J.J. Harou, Multiobjective optimization with HEC res-PRM application to the upper Mississippi reservoir system, Oper. Reserv. Chang. Cond., Proceedings (2006) 215–224, https://doi.org/10.1061/40875(212)22.
[15] L. Ostadrahimi, M.A. Mariño, A. Afshar, Multi-reservoir operation rules: multi-swarm PSO-based optimization approach, Water Resour. (2012) 407–427, https://doi.org/10.1007/s11269-011-9924-9.
[16] A.G. Adera, K.T. Alfredsen, Climate change and hydrological analysis of Tekeze river basin Ethiopia: implication for potential hydropower production, J. Water Clim. Change. 11 (3) (2020) 744–759, https://doi.org/10.2166/wcc.2019.203.
[17] T.W. Mekonnen, S.T. Teferi, F.S. Kebede, Assessment of impacts of climate change on hydropower-dominated power system — the case of Ethiopia, Hydrology 7 (4) (2022) 98, https://doi.org/10.3390/hydrology7040098.
[18] K.B. Mirani, M.A. Ayele, T.K. Lohani, T.Y. Ukumo, Evaluation of hydropower generation and reservoir operation under climate change from Kesem Reservoir, Ethiopia, Adv. Meteorol. 2022 (2022), https://doi.org/10.1155/2022/3336257.
[19] B.T. Diriba, Surface runoff modeling using SWAT analysis in Dabus watershed, Sustain. Water Resour. Manag. 7 (6) (2021) 1–11, https://doi.org/10.1007/s40899-021-00573-1.
[20] A.A. Demissie, A.A. Solomon, Power system sensitivity to extreme hydrological conditions as studied using an integrated reservoir and power system dispatch model, the case of Ethiopia, Appl. Energy 182 (2016) 442–463, https://doi.org/10.1016/j.apenergy.2016.08.106.

[21] G.M. Bombelli, S. Tomiet, A. Bianchi, D. Bocchiola, Impact of prospective climate change scenarios upon hydropower potential of Ethiopia in GERD and GIBE dams, Water 13 (5) (2021) 716, https://doi.org/10.3390/w13050716.

[22] N.C. Emiru, J.W. Recha, J.R. Thompson, A. Belay, E. Aynekulu, A. Manyevere, T.D. Demissie, P.M. Osano, J. Hussein, M.B. Molla, G.M. Mengistu, D. Solomon, Impact of climate change on the hydrology of the upper Awash River basin, Ethiopia, Hydrology 9 (1) (2022) 3, https://doi.org/10.3390/hydrology9010003.

[23] T.F. Merga, Development of water allocation and utilization system for Koka reservoir under climate change and irrigation development scenarios: a case study of upper Awash, Ethiopia, Int. J. Environ. Sci. 9 (4) (2020) 109–116. http://www.crdeepjournal.org/wp-content/uploads/2020/11/Vol-9-4-3-IJES.pdf.

[24] O.W. Owino, O. Christopher, D. Simeon, O. Lydia, An analytical assessment of climate change trends and their impacts on hydropower in Sondu Miriu River Basin, Kenya, Afr. J. Environ. Sci. Technol. 15 (12) (2021) 519–528, https://doi.org/10.5897/AJEST2021.3064.

[25] S.D. Abdulahi, B. Abate, A.E. Harka, S.B. Husen, Response of climate change impact on streamflow: the case of the Upper Awash sub-basin, Ethiopia, J. Water Clim. Change 13 (2) (2022) 607–628, https://doi.org/10.2166/wcc.2021.251.

[26] S.W. Halcrow, Master Plan for the Development of Surface Water Resources in the Awash Basin, 1989. https://www.semanticscholar.org/paper/Master-Plan-for-the-Development-of-Surface-Water-in-Halcrow/995707ccdaae031dd2eb670b8efca1aa3807dab0. (Accessed 23 September 2021). Accessed.

[27] P. Shimels, Establishing Water Release Rule Curve for Koka Reservoir for Wet Seasons, Master thesis, Addis Abeba University, Ethiopia, 1998. http://thesisbank.jhia.ac.ke/id/eprint/7519. Accessed 12 June 2022.

[28] N. Kefyalew, K. Tadele, M.K. Leta, Simulation and Optimization for Operation of Koka Reservoir, Master Thesis, Jimma University, Jimma, Ethiopia, 2017. https://repository.ju.edu.et/bitstream/handle/123456789/7367/nati%20Research%20pdf%20after%20final%20de%201.pdf?sequence=1&isAllowed=y. (Accessed 21 December 2021). Accessed.

[29] E.A. Heyi, M.O. Dinka, M. Girma, Assessing the impact of climate change on water resources of upper Awash River sub-basin, Ethiopia, J. Water Land Dev. 52 (1–3) (2022) 232–244, https://doi.org/10.24425/jwld.2022.140394.

[30] M. Jehanzaib, M.N. Sattar, J.H. Lee, T.W. Kim, Investigating effect of climate change on drought propagation from meteorological to hydrological drought using multi-model ensemble projections, Stoch. Environ. Res. Risk Assess. 34 (2020) 7–21, https://doi.org/10.1007/s00477-019-01760-5.

[31] S. Doulabian, S. Golian, A.S. Toosi, C. Murphy, Evaluating the effects of climate change on precipitation and temperature for Iran using RCP scenarios, J. Water Clim. Change 12 (1) (2021) 166–184, https://doi.org/10.2166/wcc.2020.114.

[32] A.D. Assamnew, G.M. Tsidu, The performance of regional climate models driven by various general circulation models in reproducing observed rainfall over East Africa, Theor. Appl. Climatol. 142 (3–4) (2020), https://doi.org/10.1007/s00704-020-03357-3.

[33] M. Faramarzi, K.C. Abbaspour, S.A. Vaghefi, M.R. Farzaneh, A.J. Zehnder, R. Srinivasan, H. Yang, Modeling impacts of climate change on freshwater availability in Africa, J. Hydrol 480 (2013) 85–101, https://doi.org/10.1016/j.jhydrol.2012.12.016.

[34] D.T. Reda, A.N. Engida, D.H. Asfaw, R. Hamdi, Analysis of precipitation based on ensembles of regional climate model simulations and observational databases over Ethiopia for the period 1989–2008, Int. J. Climatol. 35 (6) (2015) 948–971, https://doi.org/10.1002/joc.4029.

[35] W.T. Dibaba, T.A. Demissie, K. Miegel, Watershed hydrological response to combined land use/land cover and climate change in highland Ethiopia: finchaa catchment, Water (Switzerland) 12 (6) (2020) 1801, https://doi.org/10.3390/w12061801.

[36] T.A. Demissie, C.H. Sime, Assessment of the performance of CORDEX regional climate models in simulating rainfall and air temperature over southwest Ethiopia, Heliyon 7 (8) (2021), e07791, https://doi.org/10.1016/j.heliyon. 2021.e07791.

[37] S.S. Fanta, M.B. Yesuf, S. Saeed, S. Bhattacharjee, M.S. Hossain, Analysis of precipitation and temperature trends under the impact of climate change over ten districts of jimma zone, Ethiopia, Earth Syst. Environ. (2022) 1–8, https://doi.org/10.1007/s41748-022-00322-0.

[38] J. Schuol, K.C. Abbaspour, R. Srinivasan, H. Yang, Estimation of freshwater availability in the West African sub-continent using the SWAT hydrologic model, J. hydrol 352 (1–2) (2008) 30–49, https://doi.org/10.1016/j.jhydrol.2007.12.025.

[39] J. Ning, Z. Gao, Q. Lu, Runoff simulation using a modified SWAT model with spatially continuous HRUs, Environ. Earth Sci. 74 (2015) 5895–5905, https://doi.org/10.1007/s12665-015-4613-2.

[40] N. Tessema, A. Kebede, D. Yadeta, Modeling the effects of climate change on streamflow using climate and hydrological models: the case of the kesem sub-basin of the Awash River basin, Ethiopia, Int. J. River Basin Manag. (2020) 1–46, https://doi.org/10.1080/15715124.2020.1755301.

[41] G. Akoko, T.H. Le, T. Gomi, T. Kato, A review of SWAT model application in Africa, Water 13 (9) (2021) 1313, https://doi.org/10.3390/w13091313.

[42] T. Abebe, B. Gebremariam, Modeling runoff and sediment yield of Kesem dam watershed, Awash basin, Ethiopia, SN Appl. Sci. 1 (5) (2019) 1–13, https://doi.org/10.1007/s42452-019-0347-1.

[43] F.G. Tufa, C.H. Sime, Stream flow modeling using SWAT model and the model performance evaluation in Toba sub-watershed, Ethiopia, Model, Earth Syst. Environ. 7 (2021) 2653–2665, https://doi.org/10.1007/s40808-020-01039-7.

[44] C.H. Sime, T.A. Demissie, F.G. Tufa, Surface runoff modeling in Ketar watershed, Ethiopia, J. Sediment. Environ. 5 (2020) 151–162, https://doi.org/10.1007/s43217-020-00009-4.

[45] J.G.Arnold, J.R. Kiniry, R. Srinivasan, J.R.Williams, E.B. Haney, S.L. Neitsch, Soil and water assessment tool, input/output file documentation, version 2012, Texas Water Research Institute. Report 439, College Station, Texas, https://www.academia.edu/31732166/Input_Output_Documentation_Soil_and_Water_Assessment_Tool. Accessed 19 May 2022.

[46] K.C. Abbaspour, S. Vaghefi, R. Srinivasan, A guideline for successful calibration and uncertainty analysis for soil and water assessment: a review of papers from the 2016 international SWAT conference, Water 10 (1) (2018) 6, https://doi.org/10.3390/w10010006.

[47] A. Amin, N. Nuru, Evaluation of the performance of SWAT model to simulate stream flow of Mojo river watershed: in the upper Awash River basin, in Ethiopia, Hydrology 8 (1) (2020) 7–18, https://doi.org/10.11648/j.hyd.20200801.12.

[48] D.N. Moriasi, J.G. Arnold, M.W. Van Liew, R.L. Bingner, R.D. Harmel, T.L. Veith, Model evaluation guidelines for systematic quantification of accuracy in watershed simulations, Trans. ASABE (Am. Soc. Agric. Biol. Eng.) 50 (3) (2007) 885–900.

[49] A.K. Verma, M.K. Jha, R.K. Mahana, Evaluation of HEC-HMS and WEPP for simulating watershed runoff using remote sensing and geographical information system, Paddy Water Environ. 8 (2) (2010) 131–144, https://doi.org/10.1007/s10333-009-0192-8.

[50] D. Bekele, T. Alamirew, A. Kebede, G.M. Zeleke, A. Melesse, Modeling climate change impact on the Hydrology of Keleta watershed in the Awash River basin, Ethiopia, Environ. Model. Assess. 24 (2019) 95–107, https://doi.org/10.1007/s10666-018-9619-1.

[51] S.O. Connell, J. Harou, HEC-ResPRM, Perspective Reservoir Model quick start guide Version 1.0, CPD-95a. US Army Corps of Engineers, Institute for Water Resources, Hydrologic Engineering Center (HEC), Davis, USA, https://www.scribd.com/document/149642817/CPD-95a-HEC-ResPRM-QuickStartGuide-desbloqueado. Accessed 27 Dec 2021.

[52] M.K. Leta, T.A. Demissie, J. Tränckner, Optimal operation of nashe hydropower reservoir under land use land cover change in blue nile River basin, Water 14 (10) (2022) 1606, https://doi.org/10.3390/w14101606.

[53] R.G. Allen, M. Smith, L.S. Pereira, D. Raes, J.L. Wright, Revised FAO procedures for calculating evapotranspiration: irrigation and drainage paper no. 56 with testing in Idaho, Watershed Manag. Operat. Manag. 2000 (2012) 1–10, https://doi.org/10.1061/40499, 2000)125.

[54] I.G. Pechlivanidis, B.M. Jackson, N.R. Mcintyre, H.S. Wheater, Catchment scale hydrological modelling: a review of model types, calibration approaches, and uncertainty analysis methods in the context of recent developments in technology and applications, Glob. Nest J. 13 (3) (2011) 193–214, https://doi.org/10.30955/gnj.000778.

[55] N. Kannan, S.M. White, F. Worrall, M.J. Whelan, Sensitivity analysis and identification of the best evapotranspiration and runoff options for hydrological modelling in SWAT-2000, J. Hydrol 332 (3–4) (2007) 456–466, https://doi.org/10.1016/j.jhydrol.2006.08.001.

[56] D. Halwatura, M.M.M. Najim, Application of the HEC-HMS model for runoff simulation in a tropical catchment, Environ. Model. Software 46 (2013) 155–162, https://doi.org/10.1016/j.envsoft.2013.03.006.

[57] S.O. Kwakye, Quantification of the hydrological consequences of climate change in a typical West African catchment using flow duration curves, J. Water Clim. Change 13 (1) (2022) 26–42, https://doi.org/10.2166/wcc.2021.147.